Spatial variations in leaching of a low-grade, low-porosity chalcopyrite ore identified using X-ray µCT

Authors

Marijke A Fagan-Endres* [a,b]

marijke.fagan-endres@uct.ac.za

Johannes J Cilliers [c]

Andrew J Sederman [a]

Susan TL Harrison [b]

[a] Department of Chemical Engineering and Biotechnology, University of Cambridge, Pembroke Street, Cambridge, CB2 3RA, UK

[b] Centre for Bioprocess Engineering Research, Department of Chemical Engineering, University of Cape Town, Rondebosch, 7701, South Africa, Tel: +27 21 6501806

[c] Department of Earth Science and Engineering, Royal School of Mines, Imperial College London, SW7 2AZ, UK

* Corresponding author

ABSTRACT

This study presents an investigation, using 3D X-ray micro computed tomography (μCT), into the effect of sulfide mineral position within an ore particle on leaching efficiency. Three sections of an unsaturated mini-leaching column that had been packed with agglomerated low-grade, low-porosity chalcopyrite ore and leached with an acidified ferric iron solution were imaged at different stages of a 102 day experiment. Image analysis was used to quantify changes in the mineral content and the influence on this of the mineral distance from the ore particle surface, local voidage and radial position within the column. The main factor affecting the mineral recovery was identified to be proximity of the mineral to the ore particle surface, with recovery decreasing with increasing distance from the ore surface. A maximum leaching penetration was observed to exist at 2 mm from the surface, beyond which no recovery was achieved. Higher recoveries at the column wall indicated that preferential flow in this higher voidage had an additional, albeit smaller, impact on leaching efficiency.

Keywords: Leaching, X-ray μCT, surface leaching, hydrology, penetration, chalcopyrite

1. INTRODUCTION

Heap leaching is a low-cost mineral beneficiation method, commonly used to process low grade sulfidic mineral ores. In this unsaturated process, mineral recovery is facilitated when ferric ions and protons in the lixiviant come into contact and react with the mineral sulfide. This liberates the metal into solution whereby it is transported out of the heap. A key advantage of the process over conventional extraction techniques is that cost and energy requirements are decreased by the absence of fine milling of the ore, with heaps typically constructed with coarsely crushed (≤ 19 mm (Brierley, 2008)) or run-of-mine (ROM) ore. However, this means that some mineral remains located within the ore particles, distant from the surface. Because contact between the lixiviant and mineral is required for leaching, unexposed minerals may be slow to leach or unrecoverable. This issue consequently has the potential to limit heap recoveries and so should be taken into account in the design of heap operations. Investigation into this micro-scale phenomenon has previously been limited by the available traditional 'black-box' heap monitoring techniques, but recent development of micro-scale 3D imaging procedures for leaching systems now makes a comprehensive study possible.

X-ray micro computed tomography (μCT) is a well-established technique for the 3D non-invasive, non-destructive imaging of opaque samples. Though primarily developed and used as a medical imaging technique, it can be a useful tool for the study of chemical engineering systems. Already in the field of heap bioleaching it has been used in various studies. On a macro-scale Lin et al. (2005) and Yang et al. (2008) used X-ray μCT to study voidage changes that resulted from the slumping of ore beds. It has also been used on the micro-scale to monitor the structure of ore particles and mineral grains. These micro-scale studies are possible because the mineral grains have a higher X-ray absorbance than the supporting gangue material and so appear as brighter areas in the images. Miller et al. (2003) used this principle to study the effect that the crush size of the ore has on the distribution of exposed versus internal mineral grains. The findings were related to the recoveries achieved when different particle size samples were leached. They proposed that such studies could be used in the future to identify the optimal crush size of the ore with respect to mineral recovery. More recently, Ghorbani et al. (2011a,b) used X-ray μCT to study crack and mineral dissemination in sphalerite ore particles in a fully submerged system. Their porosity measurements compared well with traditional methods and they found that X-ray μCT was a more robust tool for the measurement of the spatial distribution of surface and interior micro-cracks in large ore particles than physical gas adsorption and porosimetry methods. They subsequently used their method to study the effect of comminution (crushing) devices, specifically high pressure grind rolls (HPGR) and conventional cone crushers, on the generation of cracks in the ore. Kodali et al. (2011) performed a similar X-ray μCT study, which compared HPGR to jaw-crushing. Through analysis of the images they determined that HPGR caused more particle damage, which resulted in higher copper recoveries compared to ore of the same particle size that had been prepared using the other technique. Like Miller et al. (2003), they found that grain exposure and consequently

mineral recovery decreased with an increase in particle size. Lin and Garcia (2005) used X-ray μCT to study the evolution of specific mineral grains over the course of a 67 day acid leach. They also determined the speciation of the minerals within the ore by determining the density and the effective atomic number of the minerals present in the ore and comparing the results to that of standard samples. Ghorbani et al. (2013) and Lin et al. (2016a, 2016b) have used 3D X-ray μCT coupled with kinetic models to interrogate the oft-used assumption of the shrinking core model applicability to describe leaching kinetics from ore particles, instead finding that the spatial and size distribution of the grains do impact the apparent leach kinetics.

The aim of this paper is to build on these studies and relate the recovery of mineral in a long term ferric leach of a low-grade, low-porosity chalcopyrite ore sample under unsaturated flow conditions to both the location of the mineral grains within the ore particles as well as their position within the column, thereby interrogating the ability of leaching solution to access and therefore recover value from sub-surface mineral grains in ore particles.

2. EXPERIMENTAL

2.1. Ore column preparation

Chilean Escondida low grade copper ore was used whose bulk sample mineralogy was 0.69% Cu, 2.95% Fe, 2.02% S by weight. The gangue comprised predominately of quartz, muscovite and kaolinite. The sulfide minerals were mainly present as pyrite (4 wt%) and copper sulfides (1 wt%), with the copper found mainly as chalcopyrite (29%), covellite (26%), chalcocite (25%) and bornite (12%). The overall particle size distribution (PSD) is given in Table 1 and the average internal porosity was 4.6%.

The ore was acid agglomerated as described by van Hille et al. (2010) and packed into a mini-column which was 220 mm high (total external) and had an internal diameter of 23.5 mm. A layer of filter paper followed by mesh was laid between the irrigation point and the ore to ensure that the liquid distribution was uniform across the column width. Ball bearings were attached to the outside of the column for image registration (alignment). The column was drip irrigated with a ferric solution of 5 g L^{-1} Fe^{3+} (in the form of $Fe_2(SO_4)_3$) in 0.1 M H_2SO_4 (pH 1.5) from the top at a rate of 4 mL h^{-1} (approximately 9 L m^{-2} h^{-1}) and operated at ambient temperature for a period of 102 days.

Table 1. PSD of the low grade copper ore.

Size (mm)	Weight (%)
> 16.0	6.7
8.00 – 16.0	4.6
5.60 – 8.00	47.5
2.00 – 5.60	9.4
1.18 – 2.00	13.5

0.25 – 1.18	9.9
< 0.25	8.4

2.2. X-ray µCT imaging

The X-ray µCT imaging was performed on a laboratory GE Phoenix-v|tome system, with an accelerating voltage of 100kV and a current of 70µA. For each 3D scan 600 projections were collected at 0.6º angular increments on a 1015×512 pixel detector. The targeted image resolution was 34 µm/pixel. Filtered back projection reconstruction was performed using the GE Phoenix proprietary software.

The entire ore containing region of the column was imaged before leaching was commenced. It was imaged in 11 separate sections of approximately 17.5 mm height, from top (1) to bottom (11) as shown in Figure 1, because a smaller field of view (FOV) permitted a higher image resolution. Three sections (2, 6 and 10) were selected to be monitored over the leaching period. The sections were chosen as they were spread out along the column length and initial visual inspection identified them as containing ore particles of suitable sulphide mineral content and distribution for the study. Sections 6 and 10 in particular contained large particles of interest. The sections will be henceforth referred to as section A (2), B (6) and C (10). The column was briefly taken off line (irrigation paused) to be imaged on day 0, 1, 7, 28, 40, 50, 64, 78, 88 and 102. Some scans were omitted from the final analysis due to issues with the quality (noise or poor contrast) or because differences in image resolution did not allow for accurate comparison.

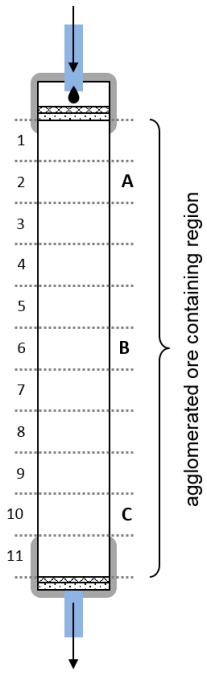

Figure 1. Schematic of the column, which gives the positions of the 11 imaging sections and shows the corresponding sections A, B and C which were monitored over the course of the leach experiment.

2.3. Image analysis

Slices 41 to 396 of the 512 slice acquisition were selected for analysis, thereby omitting boundary information that contained ring artefacts. ImageJ (Schneider et al, 2012) was used for the initial slice selection and to convert the images from 32 bit real to 8 bit images to allow for faster image analysis. The remainder of the image analysis was performed using MATLAB® (MATLAB 7.8, 2009). The images were thresholded on 2 signal magnitude levels based on a histogram analysis, as illustrated in Figure 2. The lower threshold level was used to define the total solid ore region relative to the image background. This lower threshold level was readily identified and easy to implement. The upper threshold level was used to define the sulfide mineral position within the ore. The correct threshold level to select for the sulfide minerals was more difficult to identify due to the smaller relative difference in the X-ray absorption by the gangue and sulfide minerals. To account for this, pixels with a signal magnitude one unit more or less than the upper threshold level were included in the analysis as an error measurement. The sulfide minerals identified using the upper thresholding level were not further speciated and it was assumed that variation in the mineral composition on aggregate (in each section) was not significant. Note that for brevity, the sulfide minerals identified by the upper thresholding level will henceforth be generally referred to as 'mineral', with the other ore components referred to as 'gangue'.

The resulting thresholded images, an example 2D slice of which is shown in Figure 2(b), were used to quantify the voidage and the mineral content. A region of interest was defined in this calculation which included everything within the walls of the column to avoid inclusion of any signal from the ball bearings. A morphological thinning algorithm (Baldwin et al., 1996) was used to determine the position of the mineral in the ore relative to the particle surface.

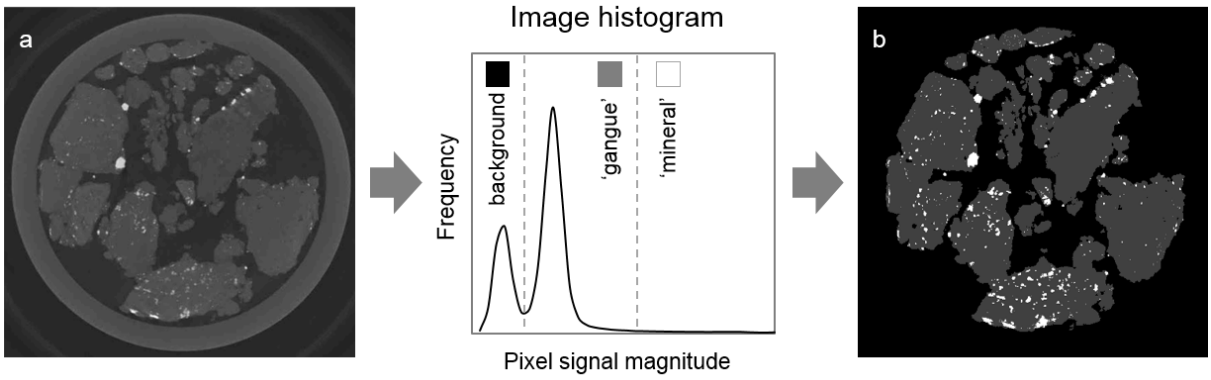

Figure 2. Example of an (a) original X-ray μCT slice from section A on day 0 whose histogram is used to create (b) its thresholded equivalent, thereby identifying the position of the sulfide 'mineral' (white) and the gangue (grey) while excluding information from outside the ore containing region. Note that

the frequency of the sulfide mineral pixels is much lower than for the other regions, making their selection comparatively more difficult.

3. RESULTS AND DISCUSSION

3.1. Overall sulfide mineral leaching

The volumetric mineral content changes over time in the three sections of the column as calculated from the thresholded 3D acquisitions are shown in Figure 3. The lowest initial total mineral content was recorded in section A (166 mm^3) while sections B and C started with similar higher mineral volumes (194 and 209 mm^3 respectively). The majority of the leaching in all of the sections occurred within the first 28 days of operation, with the leaching rate decreasing with time as the more readily recoverable mineral was removed. The overall mineral recovery (amount leached on a volumetric basis) after 102 days was 39±2%, 32±3% and 38±4% in sections A, B and C respectively. Hence slight differences in the mineral leaching existed despite the three sections having been exposed to the same leaching conditions. Two key factors were identified as possible causes of these differences: (1) variations in the packed bed structure that would affect the liquid flow path and (2) the location of the mineral grains within the ore particles.

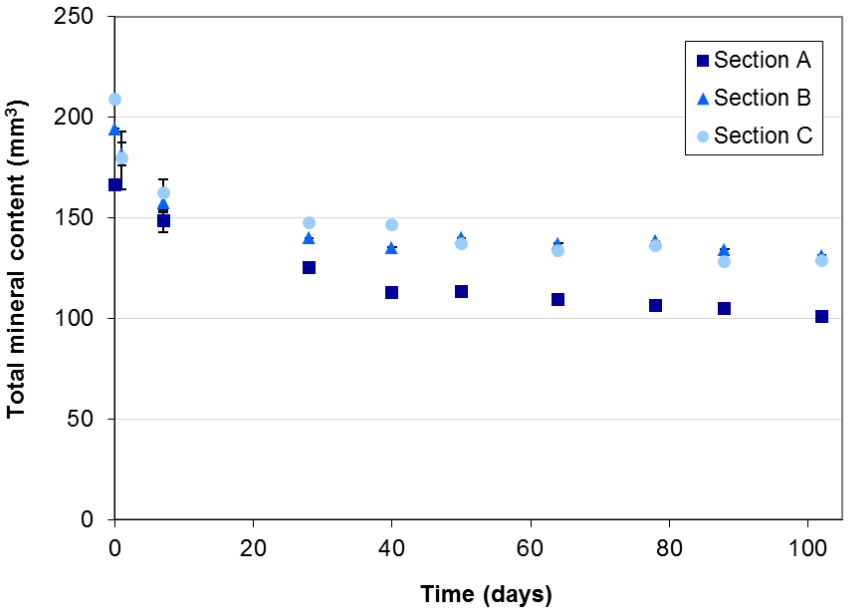

Figure 3. Changes in total volumetric sulfide mineral content in section A, B and C over time.

3.2. Voidage

The voidages of the three sections were calculated from the thresholded images to be 35.6±0.5%, 34.0±0.6% and 31.3±0.6% respectively. Insignificant variation over time (considering the error margin) was observed. This is slightly lower than has typically been quoted for heap leaching beds of comparable PSD where the voidage is circa 40% (Bouffard and Dixon, 2001; Lin et al., 2005). This deviation from the norm was because the bed was carefully packed to include as many ore particles in the sample as possible. The column is also much smaller than typical beds (to allow for a higher X-ray CT imaging resolution) in which a range of voidages would be expected to be present, including regions of low voidage comparable to this sample. No correlation between these values and the recoveries in the different sections was evident.

3.3. Mineral position in the ore

The distributions of the mineral filled voxels within the ore expressed as the distance from the ore particle surface on day 0, 7, 28, 64 and 102 are shown in Figure 4. The position of the mineral voxels and the final recovery as a function of their position are summarised in Table 2.

In the fresh ore (day 0) the majority of the mineral was positioned within 0.5 mm of the ore particle surface in all three sections. A peak in the mineral population was observed at a distance of approximately 0.07 mm (or 2 pixels) from the ore particle edge in all three cases, which may be indicative of partial volume effects at the ore surface. In section A the mineral was located a maximum of 4 mm from the ore particle surface, consistent with being centrally located in the most abundant ore particle size (5.6 – 8 mm). There was a longer tail in the mineral position distribution for section B, with some mineral located as far as 7.1 mm from the surface. Similarly, section C contained mineral a maximum of 6.1 mm from the ore surface. The larger maximum distances in sections B and C were due to large particles being contained in these regions of the column. These sections also had a larger percentage of the mineral positioned further than 2 mm from the ore surface. This is in agreement with Miller et al. (2003) who found that the amount of mineral exposed on the ore surface increases with decreasing particle size.

The highest recovery was of the mineral particles immediately on the ore surface, where 70%, 73% and 67% of the mineral is leached over the 102 day period in sections A, B and C respectively. The mineral recovery then decreased as the distance from the surface increased until there was negligible change in the mineral content located further than 2 mm from the ore surface. The position of the mineral within the ore therefore had a measureable impact on the mineral recovery, with the overall recovery increasing as the percentage of the mineral within 2 mm of the ore surface increases.

The preferential leaching of surface mineral is expected since the leaching rate of mineral from ore is dependent on the mineral surface area that comes into contact with the leaching solution (Petersen, 2010). Recent studies have reported that leaching, especially from large particles, occurs only at the

surface and subsurface regions in the ore particle, where subsurface refers to those mineral nodes that are accessible through cracks and pores (Ghorbani et al., 2011a). Mineral grains on or close to the ore particle surface are more likely to come into contact with the leaching solution, thereby increasing their chance of recovery whereas mineral not connected with the ore surface is more difficult to recover as they are less likely to come into contact with the leaching solution. The decreasing overall rate of mineral recovery with time may therefore be attributed to the fast depletion of readily contactable mineral at or near the ore surface. This corresponds with the findings of Lin et al. (2016), who demonstrated the prevalence of diffusion limited leaching characteristics further from an ore particle surface.

A greater variation in recovery with increasing distance from the ore surface was also observed. This is because the leaching of mineral further from the ore surface is more dependent on its environment, such as whether it is in contact with leachable mineral closer to the surface or is in contact with a crack.

This information may also be conceived as changes in the average distance of the mineral from the ore surface, as presented in Figure 5. Sections A and C had similar initial average distances, 0.72 mm and 0.76 mm, while section B had an initial average value of approximately 0.94 mm. The average distances increased with time in sections B and C due to the effect of preferential leaching of the surface mineral. However, only a small change in the average distance of the mineral from the ore surface was observed for section A. This was because mineral located further than 2 mm from the surface accounted for only a small percentage in this section and the maximum distance mineral was positioned from the ore surface was significantly less than in sections B and C.

Table 2. Sulfide mineral distribution and recovery as a function of the distance of the mineral from the ore particle surface in the three sections.

	Section A	Section B	Section C
Mineral position on day 0			
At & < 1 mm from surface	72%	66%	70%
1 - 2 mm from surface	22%	21%	20%
> 2 mm from surface	6%	13%	10%
Mineral recovery			
At surface	70 ± 1%	73 ± 2%	67 ± 3%
< 1 mm from surface	42 ± 1%	47 ± 2%	53 ± 3%
1 - 2 mm from surface	33 ± 4%	19 ± 2%	24 ± 1%
> 2 mm from surface	< 1%	< 1%	< 1%

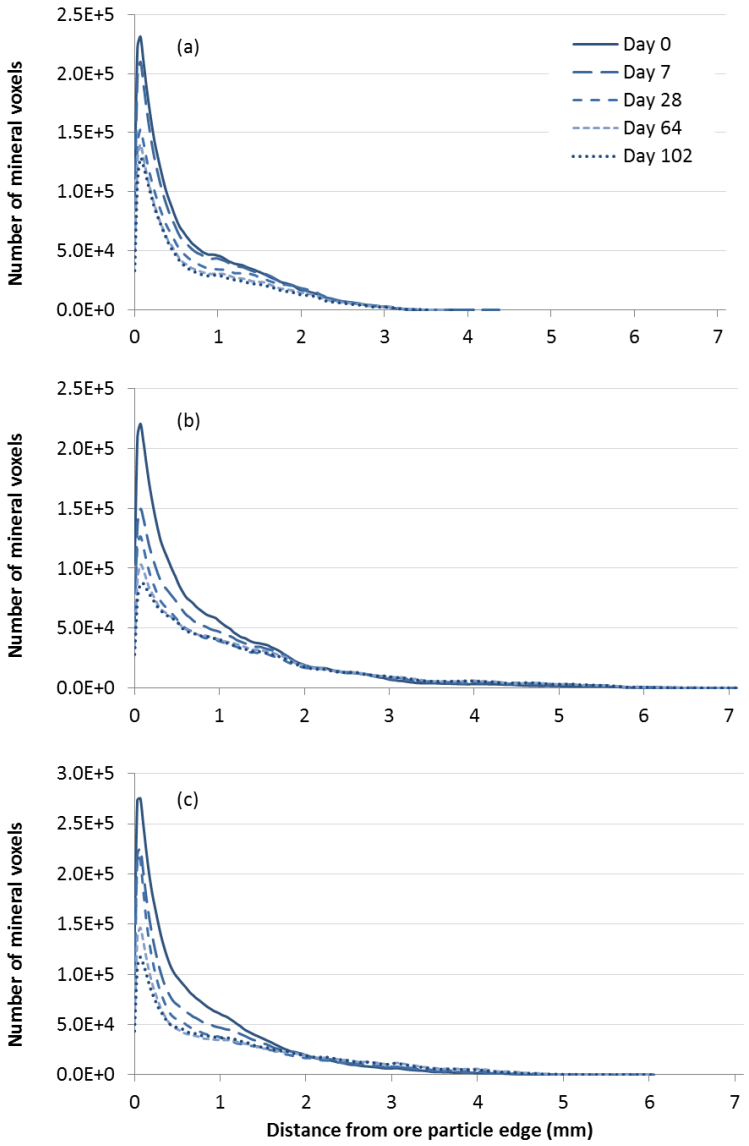

Figure 4. Change in the distribution of the sulfide mineral filled voxels as a function of time in section (a) A, (b) B and (c) C.

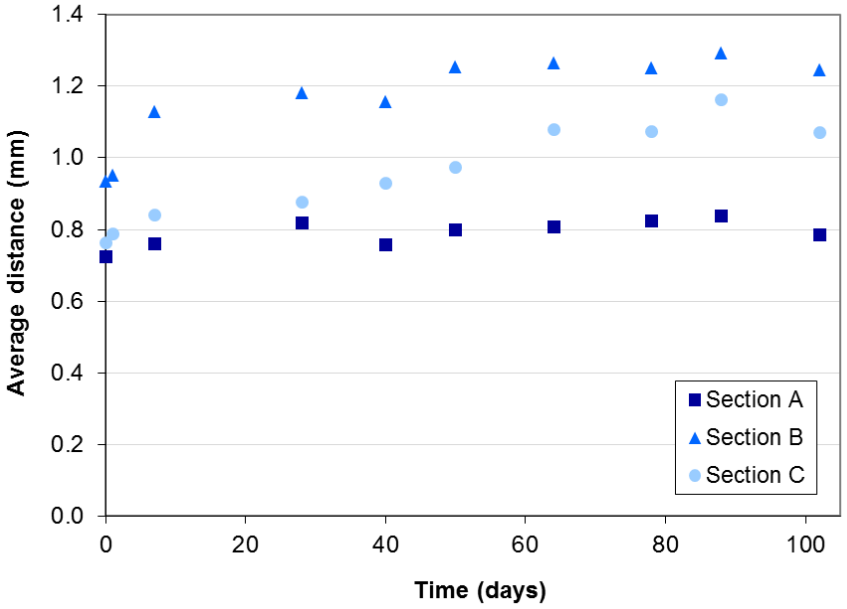

Figure 5. Average distance of the sulfide mineral from the edge of the ore particles as a function of time in section A, B and C.

3.4. Radial variations

The mineral leaching varied as a function of distance from the centre of the column as is shown in Figure 6. The highest recovery in all three sections occurred in the outermost 1.5 mm, next to the column wall (50%, 50% and 58% in A, B and C respectively). The recovery decreases towards the centre of the column until 6.8 mm from the centre within which there is little variation.

The voidage also varied as a function of radial distance from the centre of the column as is shown in Figure 7. This is a common characteristic of packed beds as particles must conform to the curvature of the column wall (Benenati and Brosilow, 1962). The highest voidage in all three sections was at the wall of the column (64±8%, 61±6% and 55±9% in A, B and C respectively). The voidage within 10.2 mm of the centre was significantly lower, on average less than half the voidage of the outer ring. No clear trend was identifiable in this central region because variations in the voidage were caused by the random orientation of ore particles. In section B in particular there was a large standard deviation in the voidage in the central 3.4 mm of the column. This was due to the large particles known to be present in the centre of this section of the column, resulting in areas of very low and very high voidage.

The voidage and mineral leaching therefore follow a similar radial trend (decreasing towards the centre of the column). This may be because the higher voidage at the column walls may have caused the leaching solution to flow preferentially along the column walls, resulting in relatively inefficient leaching in the less irrigated centre of the column. This type of behaviour would be expected in a system

with a high flow rate (relative to the particle size distribution), when liquid will preferentially flow through a region of coarser packing (O'Kane Consultants Inc., 2000). Preferential liquid flow along the column walls was supported by visual observation.

Alternatively this could correspond to mineral exposure to the surface in different regions of the column. The original volume of mineral per cubic millimetre is presented as a function of distance from the centre of the column in Figure 8. Figure 9 shows what fraction of this mineral is within 2 mm of the ore surface as the results in Section 3.3 showed that this was the mineral that was preferentially recovered. In sections B and C the fraction of mineral within 2 mm of the ore surface decreased towards the centre of the column, with the exception of the central 3.4 mm radius circle in section C where it increases. This was because of the large particles in these sections of the column whose edges, and so too the mineral within 2 mm of the ore surface, were located nearer to the walls of the column. This trend is complementary to the decrease in recovery from the outside to the centre of the column and suggests that the radial variations in recovery is because less mineral is accessible for leaching towards the centre of the column and not due to voidage effects. However, the results for section A do not fit this trend, confirming that there were factors other than the proximity of the mineral to the ore surface that contributed to the mineral leaching efficiency. Barring the existence of a higher concentration of non-recoverable mineral in the 6.8 mm closest to the centre of section A, the decrease in recovery towards the centre of the column was therefore most likely a combination of the proximity of the mineral to the ore surface and liquid distribution variations due to preferential flow into the areas of higher voidage near the column wall.

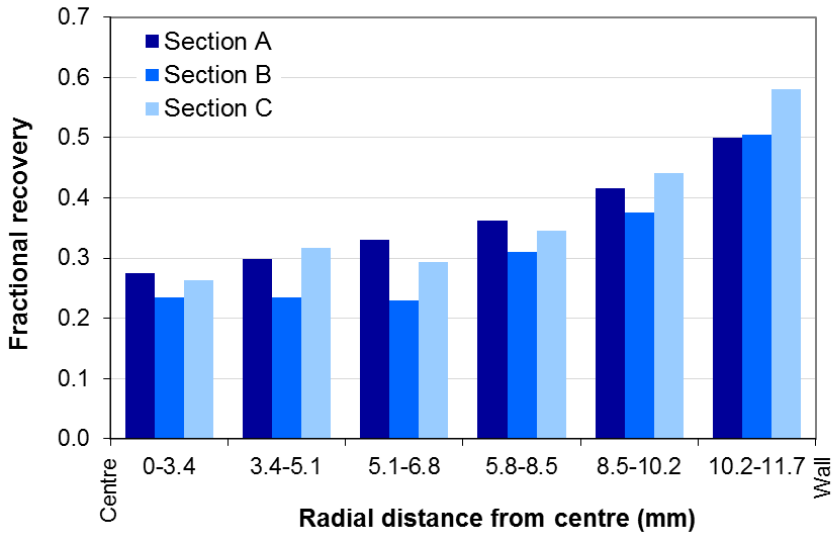

Figure 6. Recovery of the mineral after 102 days of leaching as a function of radial position in the column.

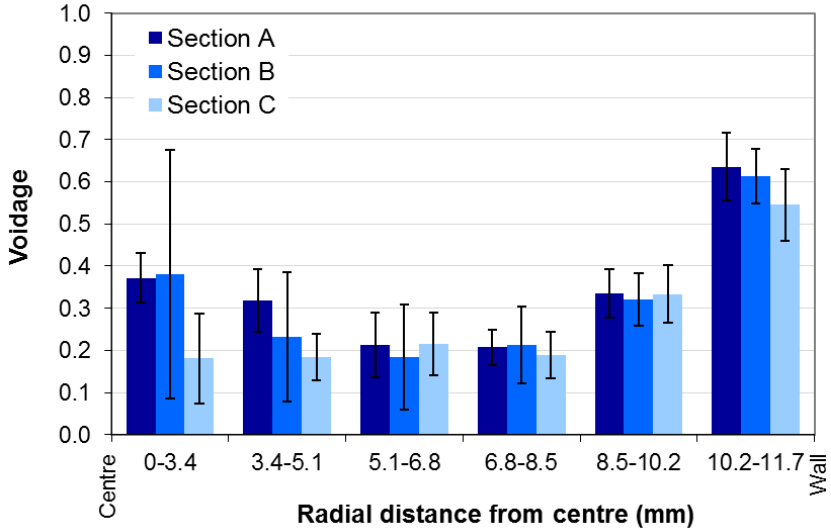

Figure 7. Radial variation in the voidage where the error bars indicate the standard deviation in the voidage in each section.

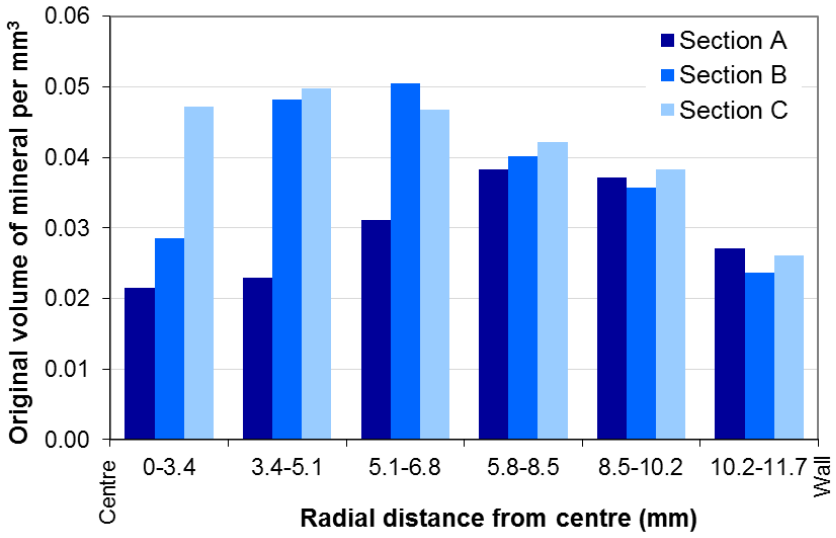

Figure 8. Volume of sulfide mineral per mm^3 on day 0 as a function of radial position in the column.

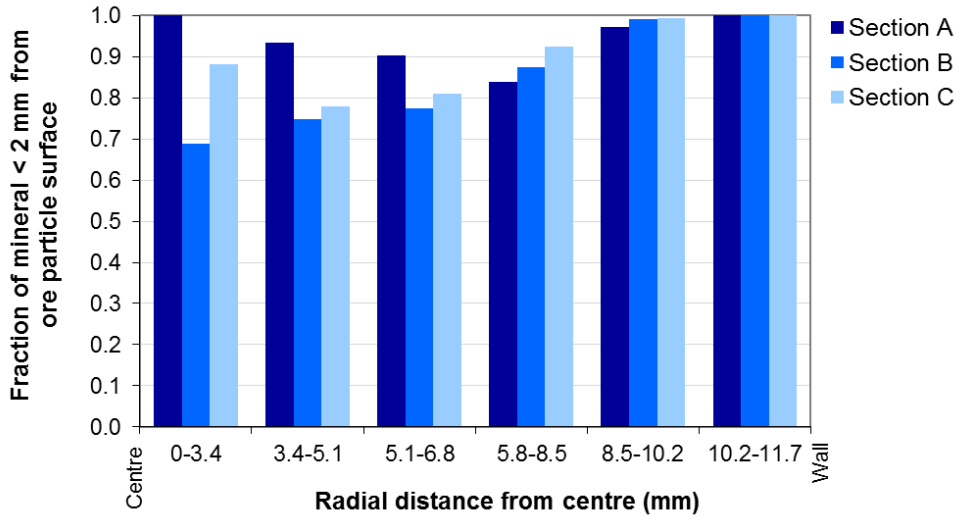

Figure 9. Fraction of the sulfide mineral particles less than 2 mm from the ore surface on day 0 as a function of radial position in the column.

4. CONCLUSIONS

The proximity of the mineral grains to the ore particle surface had a pronounced influence on recovery for this chalcopyrite ore, with leaching recoveries found to be highest on the ore particle surface and then decreasing as the distance from the ore particle surface increased. This was coupled with a higher leaching variability as the distance from the ore particle surface increased, proposed to be because the recovery of mineral located further from the ore surface has a higher dependence on the surrounding environment, such as whether it is in contact with other reactive minerals or cracks that link it to the surface. A maximum leaching penetration distance of 2 mm was observed to exist for the ore, not seen for other ores previously studied using X-ray μCT; thus showing full metal recovery is not possible with the ore in its given state. Further particle size reduction to ensure access to these mineral grains is often not practicable for heap leaching due to both increased costs as well as liquid flow issues that may result due to decreased ore bed permeability. This motivates the need to identify mechanisms for the improved permeability of the ore particles of interest, for example through the selection of appropriate comminution methods for internal crack propagation during ore preparation or through degradation of the support material during the leaching process, highlighting the importance of improved understanding of an ore's full mineralogy and the composition of the gangue.

The radial variations in the mineral leaching showed that the proximity of the mineral to the ore surface was not the only phenomenon that affected mineral recovery. The high recovery at the column wall was attributable to preferential flow of the leaching solution in the higher voidage regions at the column wall. Therefore variations in inter-particle pore size (voidage) effected through preferential liquid flow paths were found to have some influence on the mineral recovery. Further investigations into the effect

of liquid distribution and flow on mineral leaching are being pursued using a combined Magnetic Resonance Imaging (MRI) – X-ray μCT approach.

Acknowledgements

The authors would like to acknowledge and thank BHP Billiton, the Cambridge Commonwealth Trust and the South African Research Chairs Initiative of the Department of Science and Technology for their sponsorship and support of this project. We also thank Dr Áine Ní Bhreasail, Dr Kathryn Hadler, Dr Saied Moradi and Prof Peter Lee for the image acquisition and processing at Imperial College London.

REFERENCES

Baldwin, CA, Sederman, AJ, Mantle, MD, Alexander, P and Gladden, LF (1996) Determination and characterization of the structure of a pore space from 3D volume images, *J. Colloid Interface Sci.*, 181(1), 79-92.

Benenati, RF and Brosilow, CB (1962) Void fraction distribution in beds of spheres, *AIChE J.*, 8(3), 359-361.

Brierley, CL (2008) How will biomining be applied in future?, *Trans. Nonferrous Met. Soc. China*, 18, 1302-1310.

Bouffard, SC and Dixon, DG (2001) Investigative study into the hydrodynamics of heap leaching processes, *Metall. Mater. Trans. B*, 32(5), 763-776.

Ghorbani, Y, Becker, M, Mainza, A, Franzidis, JP and Petersen, J (2011a) Large particle effects in chemical/biochemical heap leach processes – A review, *Miner. Eng.*, 24(11), 1172-1184.

Ghorbani, Y, Becker, M, Petersen, J, Morar, SH, Mainza, A and Franzidis, JP (2011b) Use of X-ray computed tomography to investigate crack distribution and mineral dissemination in sphalerite ore particles, *Miner. Eng.*, 24(12), 1249-1257.

Ghorbani, Y, Petersen, J, Becker, M, Mainza, AN and Franzidis, JP (2013) Investigation and modelling of the progression of zinc leaching from large sphalerite ore particles, *Hydrometallurgy*, 131-132: 8-23.

Kodali, P, Dhawan, N, Depci, T, Lin, CL and Miller, JD (2011) Particle damage and exposure analysis in HPGR crushing of selected copper ores for column leaching, *Miner. Eng.*, 24(13), 1478-1487.

Lin, CL and Garcia, C (2005) Microscale characterization and analysis of particulate systems via cone-beam X-ray microtomography (XMT), in: Young, C. A., Kellar J.J., Free, M.L., Drelich, J., King, R.P. (Eds.), *Innovations Nat. Resour. Process., Proc. Jan D. Miller Symp.*, Society for Mining, Metallurgy and Exploration, 421-432.

Lin, CL, Miller, JD and Garcia, C (2005) Saturated flow characteristics in column leaching as described by LB simulation, *Miner. Eng.*, 18(10), 1045-1051.

Lin, Q, Barker, DJ, Dobson, KJ, Lee, PD and Neethling, SJ (2016a) Modelling particle scale leach kinetics based on X-ray computed micro-tomography images, *Hydrometallurgy*, 162, 25-36.

Lin, Q, Neethling, SJ, Courtois, L, Dobson, KJ and Lee, PD (2016b) Multi-scale quantification of leaching performance using X-ray tomography, *Hydrometallurgy*, 164, 265-277.

MATLAB 7.8 (2009) The MathWorks, Inc., Natick, Massachusetts, United States.

Miller, JD, Lin, CL, Garcia, C and Arias, H (2003) Ultimate recovery in heap leaching operations as established from mineral exposure analysis by X-ray microtomography, *Int. J. Miner. Process.*, 72(1–4), 331-340.

O'Kane Consultants Inc. (2000) Demonstration of the application of unsaturated zone hydrology for heap leaching optimization, *Industrial Research Assistance Program Contract # 332407*, (628-1).

Petersen, J (2010) Modelling of bioleach processes: Connection between science and engineering, *Hydrometallurgy*, 104(3-4), 404-409.

Schneider, CA, Rasband, WS, Eliceiri, KW (2012) NIH Image to ImageJ: 25 years of image analysis, *Nature Methods*, 9(7): 671-675.

van Hille, RP, van Zyl, AW, Spurr, NRL, Harrison, STL (2010) Investigation heap bioleaching: Effect of feed iron concentration on bioleaching performance, *Miner. Eng.*, 23(6) 518-525.

Yang, BH, Ai-Xiang, W, Jiang, HC and Chen, XS (2008) Evolvement of permeability of ore granular media during heap leaching based on image analysis, *Trans. Nonferrous Met. Soc. China*, 18(2), 426-431.